Eur. Phys. J. B (2016) 89: 142
DOI: 10.1140/epjb/e2016-60886-y

THE EUROPEAN PHYSICAL JOURNAL B

Regular Article

Structural and electronic properties of solid naphthalene under pressure: density functional calculations

Ling-Ping Xiao[1,2,a], Zhi Zeng[1,2,b], and Xiao-Jia Chen[1,3]

[1] Key Laboratory of Materials Physics, Institute of Solid State Physics, Chinese Academy of Sciences, Hefei 230031, P.R. China
[2] University of Science and Technology of China, Hefei 230026, P.R. China
[3] Center for High Pressure Science and Technology Advanced Research, Shanghai 201203, P.R. China

Received 4 November 2015 / Received in final form 23 January 2016
Published online 6 June 2016 – © EDP Sciences, Società Italiana di Fisica, Springer-Verlag 2016

Abstract. The pressure effect on the geometrical and electronic structures of crystalline naphthalene is calculated up to 30 GPa by performing density functional calculations. The lattice parameters a, b, and c, decrease by 1.77 Å (–20.4%), 0.85 Å (–14.1%), and 0.91 Å (–8.2%), respectively, while the monoclinic angle β increases by 3.95° in this pressure region. At the highest pressure of 30 GPa the unit cell volume decreases by 62.7%. The detailed analysis of the molecular arrangement within crystal structure reveals that the molecular motion becomes more and more localized, and hints towards the evolution of intermolecular interaction with pressure. Moreover, the electronic structure of naphthalene under high pressure is also discussed. A pressure induced decrease of the band gap is observed.

1 Introduction

Molecular materials of hydrocarbons, such as fullerenes, graphite, and polycyclic aromatic hydrocarbons, built of conjugated molecules, have been extensively studied because of their exceptional properties and extensive applications [1–3]. A deeper understanding of the relationship between the geometric structure, chemical bonding, and intermolecular interaction behavior as well as electrical properties in molecular materials should promote the advancement of functional organic devices. Properties of molecular materials are also determined indeed by the subtle interplay among a number of intermolecular and intramolecular interactions [4]. Tuning intermolecular and intramolecular interactions in molecular materials is effective by applied hydrostatic pressure. In some cases, this has resulted in intriguing and unexpected physical properties, such as metallic behavior [5] and superconductivity [6,7]. Among molecular materials, naphthalene as a representative of the large class of polycyclic aromatic hydrocarbons (PAHs) has served for a long time as model compounds for organic molecular materials.

At ambient pressure, pure naphthalene crystal structure belongs to the monoclinic has space group $P2_1/a$, with two molecules in the primitive unit cell [8]. The crystal structure of solid naphthalene is shown in Figure 1. Many experimental and theoretical studies on naphthalene have attracted considerable and various interests as a function of pressure during the past decades [9–12]. The

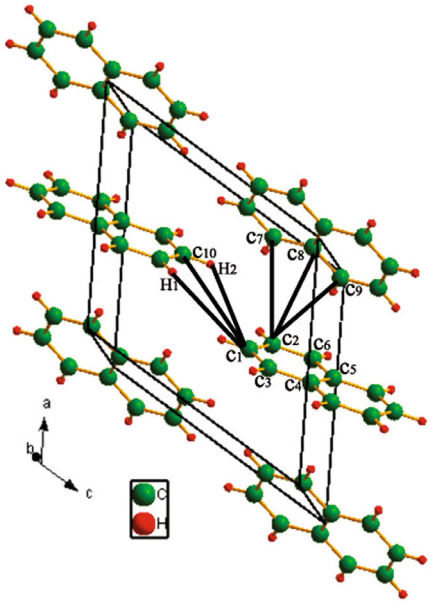

Fig. 1. Crystal structure of naphthalene.

Raman spectra of a crystalline naphthalene have been measured at room temperature in the pressure range up to 20 GPa. The Grüneisen parameters for intermolecular and intramolecular phonons have been determined [13]. Likhacheva et al. using the diffraction experiment and calculations show the initial monoclinic phase of naphthalene with the space group $P2_1/c$ ($P2_1/a$) to be stable up to at least 773 K in the pressure range of 3–15 GPa [14,15]. These authors have calculated the frequency dependence

[a] e-mail: xiaolingping1982@163.com
[b] e-mail: zzeng@theory.issp.ac.cn

on pressure and compared the results with those obtained by Meletov [13]. Meanwhile, Coropceanu et al. [16] combine density theory calculations and molecular mechanics simulations and use a chemistry-based insight to derive the nonlocal electron-phonon coupling constants due to the interaction of charge carriers with the optical lattice vibrations in the naphthalene crystal. Schatschneider et al. used density functional theory with Tkatchenko-Scheffler dispersion correction to calculate the structures and optical properties of crystalline oligoacenes, from naphthalene (2A) to pentacene (5A) [17]. These simulations report that under hydrostatic conditions there is no evidence of a structural phase transition up to 30 GPa at room temperature. High pressure has been proven to be an efficient tool for improving the understanding of the main physical properties of compounds, as the distance between atoms is effectively reduced under pressure. The electronic and optical properties of compounds with two to five aromatic rings, using first-principle methods, were studied by Hummer and Ambrosch-Draxl [18]. The mechanism of formation of chemical bonds in naphthalene and anthracene was studied by Fedorov et al. [19]. Recently, Zhuravlev et al. [20] and other authors studied electronic properties of naphthalene and the effect of hydrostatic pressure on its structure. Here, we examine the pressure dependent geometrical and electronic structures properties of naphthalene under hydrostatic pressure up to 30 GPa. The information of the pressure dependence of lattice parameters, the electronic band structure, and the energy gap are provided.

2 Computational methods

The calculations carried out in this work are based on the density functional theory (DFT) using the VASP program package [21]. The geometric structure and electronic properties were fully optimized using DFT with the generalized gradient approximation with vdW interactions treated using the vdW-DF2 correlation functional [22]. The self-consistent calculations were carried out with an $8 \times 8 \times 8$ k-point mesh. To balance accuracy and speed, the plane-wave basis set cutoff was set to 750 eV. Self-consistency calculation is achieved when the total-energy variation converged to a 0.01 meV accuracy or better.

While the DFT geometry optimizations were performed by constraining the cell parameters to experimental data with the lattice constants $a = 8.554$ Å, $b = 6.016$ Å, $c = 11.174$ Å, and $\beta = 124.60°$ in the monoclinic space group $P2_1/a$ [23]. The external pressure was gradually increased by an increment of 1 GPa. In recent years there have been studies of the effects of pressure on the crystalline structure of naphthalene, however, there are no definitive results concerning the presence or absence of phase transition. Bridgman described phase transition at 3 GPa [24]. But further investigations did not confirm this result [25]. Moreover, the first principle calculations predict the absence of phase transition at 0–30 GPa, $T = 0$ K [14,17]. Thus, during the geometry optimization, the space group of the naphthalene crystal has been constrained to $P2_1/a$. No structural phase transition will be considered in this study.

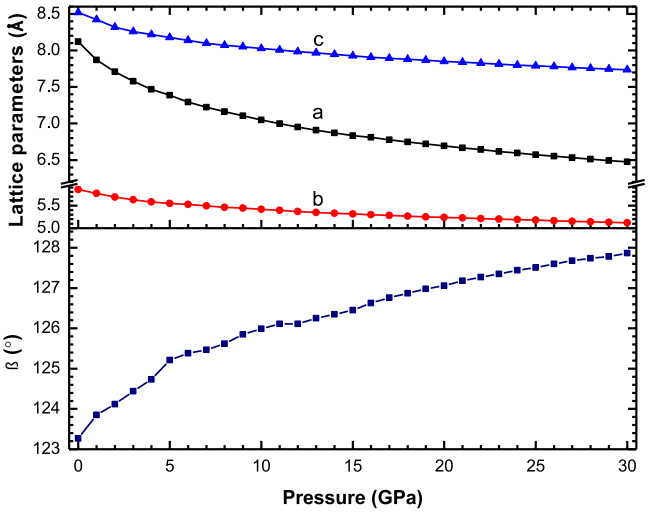

Fig. 2. The lattice parameters a, b, c, and β of naphthalene under high pressure up to 30 GPa.

3 Results and discussion

3.1 Evolution of structural properties with pressure

In order to test the reliability of the optimized geometries, we have calculated the average difference in absolute value between the experimental and calculated bond lengths and lattice parameters reported in Table 1. The overall deviations between our calculations and the experiments are less than 2% in lattice parameters and unit cell volumes. Similar agreement is also found for the internal molecular geometries, in which the vdW-DF2 method predicts the C-C distances with an accuracy of 2% in comparison with X-ray measurements [27,28]. These results point out that the vdW-DF2 method yields better bond length values for this type of aromatic hydrocarbons than the LDA/PBE method.

The pressure dependence of the lattice parameters a, b, c, and β of naphthalene are shown in Figure 2. As expected, the lattice parameter a has the strongest pressure dependence with $\Delta a = 1.65$ Å, and b and c show a pressure dependence of $\Delta b = 0.73$ Å and $\Delta c = 0.79$ Å up to 30 GPa, respectively. The monoclinic angle increases by $\Delta\beta = 4.6°$ in the same pressure region, which is due to the reduction of the lattice parameters and the associated decrease of the layer distance. All the cell parameters decrease with increasing pressure and the cell parameter a shows large change for the applied pressure. Obviously, the pressure dependence of the lattice constant a is almost twice as large as the change of the other two lattice constants b and c, which shows that the intermolecular bonding along a axis is softer and hence more easily compressible than that along other crystallographic axes. When applying a linear fitting in the lower and higher pressure

Table 1. The structural data of the crystal naphthalene under zero pressure.

C-C bond lengths (Å)	Calc. [19]	Expt. [26]	This work
C1-C2	1.413	1.407	1.413
C1-C3	1.376	1.368	1.376
C3-C4	1.416	1.424	1.415
C4-C5	1.432	1.420	1.431
C5-C6	1.416	1.419	1.416
C2-C6	1.377	1.374	1.377
Lattice parameters			
a/Å	8.190	8.213	8.221
b/Å	5.999	5.973	5.904
c/Å	8.584	8.675	8.550
β (°)	124.00	123.39	123.10
V (Å^3)	349.67	355.28	347.6

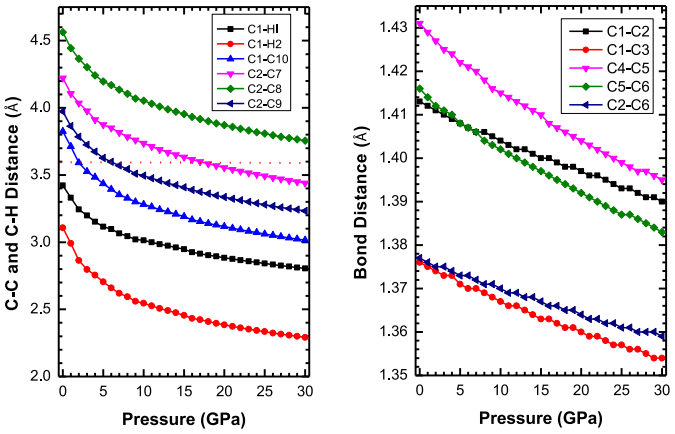

Fig. 3. Pressure dependence of the intermolecular and interatomic (covalent bonds) distances (the red dashed line marks the doubled van der Waals radius of a carbon atom [31]).

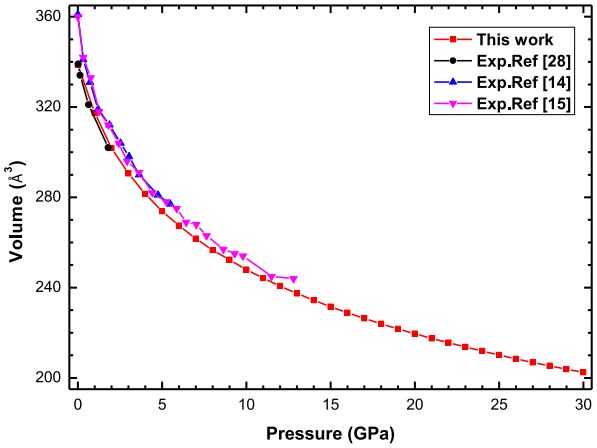

Fig. 4. The unit cell volume compressibility of naphthalene at room temperature. Experimental results are presented for comparison.

range, the linear compressibility of the lattice parameters a, b, c, is 0.14 GPa^{-1}, 0.06 GPa^{-1} and 0.07 GPa^{-1} up to 5 GPa, and from 5 to 30 GPa is 0.03 GPa^{-1}, 0.01 GPa^{-1}, and 0.02 GPa^{-1}, respectively. The nonuniform pressure dependence of the lattice parameters may imply that the sample undergoes anisotropic compression and the intermolecular interactions are anisotropically altered with pressure.

Previous investigations of the structural properties of naphthalene under pressure have revealed that within the layer the C-H$\ldots\pi$ intermolecular bonds are predominant, whereas interlayer contacts are mainly C-H$\cdots$H-C [29]. Kitaigorodski claimed that it is the individual atom which is responsible for the interactions in a molecular crystal and not the molecule as a whole [30]. The molecular arrangement in crystal structure is mostly determined by molecular conformation and intermolecular interactions. The intermolecular distances within and between the herringbone layers and interatomic (covalent bonds) distances as a function of pressure are showed in Figure 3. The dashed line marking doubled van der Waals radius with 3.6 Å is the ambient pressure interatomic distance [31]. At ambient pressure, all the shortest intermolecular C-C are larger than this value. When increasing pressure, these distances all fall below the van der Waals radii. The C-C bond lengths have the pressure dependence with $\Delta_{\text{c-c}} = 18$ mÅ, but the decrease in intermolecular C-C and C-H distances turn out to be 739–618 mÅ between 0 and 30 GPa. Comparing the pressure effect on the shortest intermolecular distances and on the bond lengths, we confirm the expected result that the intermolecular interactions are more sensitive to pressure than the intramolecular interactions. As mentioned above, the observed anisotropic high-pressure of the lattice parameters is consistent with the compression mechanism found previously for a narrower pressure range of 0–2 GPa, which includes rotation of the neighboring molecular within the herringbone pattern relative to each other, so that they become more parallel. This similar behavior was often observed in aromatic compound such as anthracene [21], benzene [32] and naphthalene dimmers [33].

Moreover, by increasing pressure, the cell volumes are readily compressed. The variation of the unit cell volume for naphthalene with pressure is shown in Figure 4.

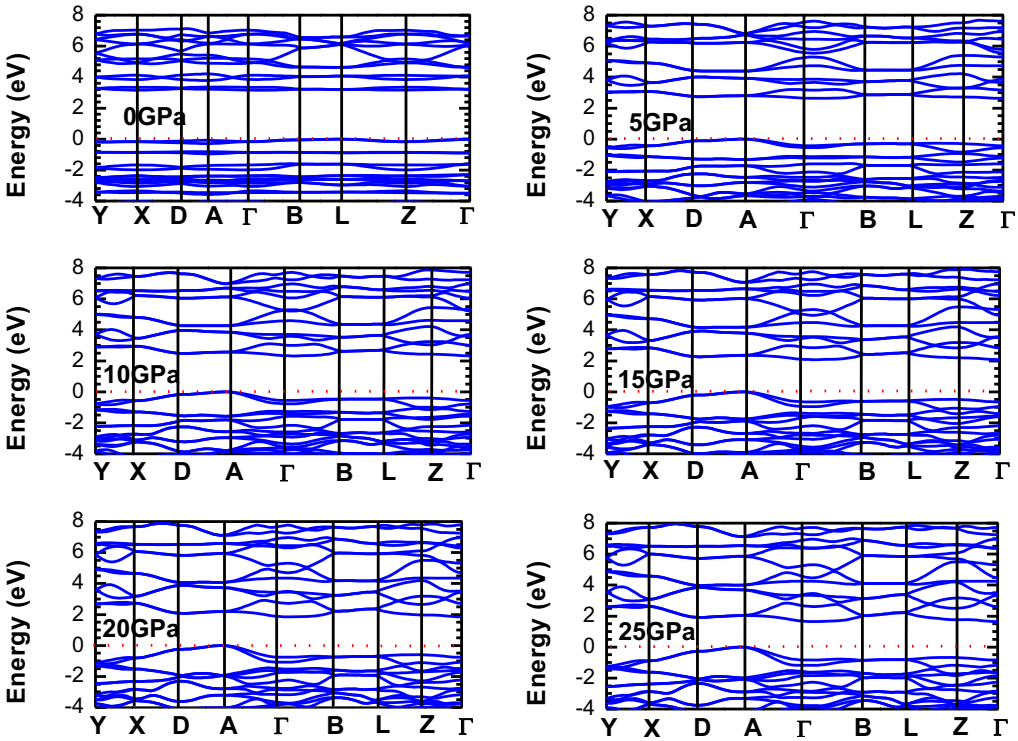

Fig. 5. The band structures of naphthalene at 0 GPa, 5 GPa, 10 GPa, 15 GPa, 20 GPa, and 25 GPa, respectively. In each case the Fermi level is indicated by a dashed line.

The red lines are the fitting results by using the third-order Birch-Murnaghan equation of state,

$$P = \frac{3}{2}B_0\left[\left(\frac{V}{V_0}\right)^{-7/3} - \left(\frac{V}{V_0}\right)^{-5/3}\right] \times \left\{1 + \frac{3}{4}\left(B_0^{'} - 4\right)\left[\left(\frac{V}{V_0}\right)^{-2/3} - 1\right]\right\},$$

where B_0 is the bulk modulus, $B_0^{'}$ is the derivative of bulk modulus at ambient pressure, and V_0 is the volume at ambient pressure. At 30 GPa the volume compression is $V/V_0 = 59.7\%$. The bulk modulus at ambient pressure and temperature is $B_0 = 10.26$ GPa and its derivative is $B'_0 = 8.18$. The low bulk modulus shows that the sample is easily to be compressed under high pressure. As the computation was performed at 0 K, the $V(P)$ dependence should be below experimental results. However, large dispersion is observed in both experimental and theoretical studies. The bulk modulus of naphthalene $B_0 = 8.4(3)$ GPa is determined in the pressure range of 0–13 GPa from the recent volumetric measurements of Likhacheva et al., which differs with the $B_0 = 8.7$ GPa estimated from the first principles calculations [14,15]. Since the unit cell volume is decreased, the intermolecular interaction between neighboring molecules and the overlap of the molecular orbitals are enhanced. Meanwhile, looking from the theoretical point of view on the pressure induced decrease of the intermolecular distances in a crystal and increase of the electron orbital overlap between adjacent molecules, one can see that this dependence has two contributions. The first contribution is due to the change of the crystal volume and the second one is due to the change of the electrical resistivity.

3.2 Electronic structure and band gap

Pressure is a tool that usually reduces the electrical resistivity mainly by enhancing the dimensionality, which might help the electron pass, avoiding the scattering site [34]. Several groups have observed the decrease of the bandwidth with increasing pressure in oligoacene crystals. Katayama et al. explained the pressure-induced zero gap semiconducting state in organic conductor salt [35]. Especially the pressure-induced increase of the intermolecular overlap results in the vanishing of the band gap, and metallization was also observed in pentacene [36]. In order to gain insight into the origin of the electronic properties, we calculated band structure for crystalline naphthalene and examined its change under hydrostatic compression. In accordance with the work of Kovalev, the high-symmetry points in units of $(\frac{2\pi}{a}, \frac{2\pi}{b}, \frac{2\pi}{c})$ are $Y = (0.5, 0, 0)$, $X = (0.5, 0, 0.5)$, $D = (0.5, 0.5, 0.5)$, $A = (0.5, 0.5, 0)$, $\Gamma = (0, 0, 0)$, $B = (0, 0.5, 0)$, $L = (0, 0.5, 0.5)$ and $Z = (0, 0, 0.5)$ [19]. Note that ΓY (ΓB) is parallel to the crystalline a axis (b axis), and TZ corresponds to the c direction, which is approximately the long molecular axis.

The band structure of naphthalene at 0 GPa, 5 GPa, 10 GPa, 15 GPa, 20 GPa, and 25 GPa is presented in Figure 5 as a representive example. As is well-known, the four

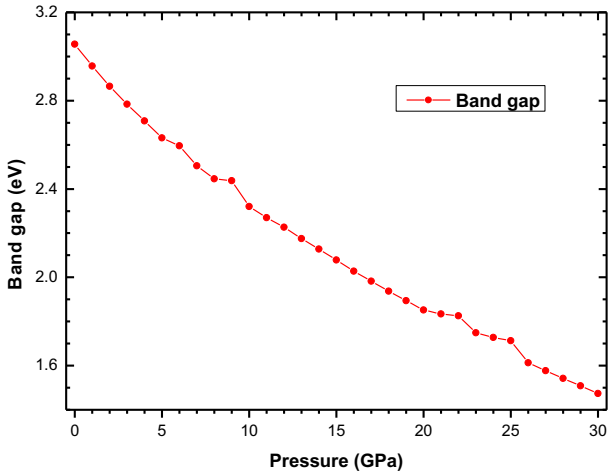

Fig. 6. The band gap of naphthalene under high pressure up to 30 GPa.

lowest lying excited electronic states deriving from states obtained by excitation of one electron from the HOMO or HOMO–1 to the LUMO or LUMO+1 molecular orbitals in the naphthalene molecule are π-electron orbitals, mixed by configuration interaction. Due to the three-dimensional effects and the π-wave functions of neighboring molecules, the main features of the band structure of naphthalene are anisotropic band dispersion and band splitting. More precisely, since the crystal structure stacked along c axis with a herringbone arrangement on the a-b plane is layered, the electronic structure is more dispersive along the $2\pi/a$-$2\pi/b$ axis. The dispersion along $2\pi/a$ is larger than that along $2\pi/b$, which directly reflects the distance between neighboring molecules being shortest along a. This is in accordance with the pressure dependence of the lattice parameter a, which is affected most by pressure.

While the top of the valence band is realized at the A point, the minimum value of the conduction band is at the Γ point in the Brillouin zone. Thus the naphthalene is predicted be an indirect band gap semiconductor. The calculated band gaps of naphthalene as functions of pressure are shown in Figure 6. As the pressure increases, the conduction and valence band shift to lower and higher energies, respectively. The shifts of the conduction and valence band result in decreasing band gap. We can see that the band gap reduces smoothly under compression without any significant discontinuity. However, in several previous works a distinct optical anomaly was detected near 3 GPa. Specifically, pressure-induced anomalies in fluorescence and phonon spectra have been detected in a variety of PAHs [37,38]. A discontinuous shift of all the bands towards higher frequencies was observed in the infrared spectrum of naphthalene in the pressure range of 2–4 GPa [39]. Conversely, a recent Raman study revealed only a minor irregularity in the dependence of the intermolecular and some intramolecular phonons on the crystal density within the same pressure range [13]. According to our calculation, the average decrease of the band gap up to 5 GPa is 0.08 eV/GPa and 0.05 eV/GPa from 5 to 21 GPa and 0.03 eV/GPa from 21 to 30 GPa, respectively. To determine the pressure coefficient, we fitted the direct band gap ($E_g(P)$) with a quadratic function: $E_g(P) = E_g(0) + mP + nP^2$, and obtained $m = -0.07$ eV/GPa and $n = 7.84$ eV/(GPa)^2.

The total density of states (DOS) and partial density of states (PDOS) of the naphthalene under 0 GPa, 5 GPa, 10 GPa, 15 GPa, 20 GPa, and 25 GPa are shown in Figure 7. The peaks of DOS for conduction and valence bands are shifted slightly to higher and lower range. And the reductions are consistent with the band structures. According to the PDOS, the valence and conduction bands near the Fermi level mainly come from C $2p$, and a strong hybridization can be found between H $1s$ state and C $2p$ state in the conduction band at the energy between 5.96 and 6.47 eV. The conduction band minimum is mainly composed of H $1s$ and C $2p$ states. But the band at the energy between 6.96 and 7.47 eV mainly comes from H $1s$. The valence band derives from H $1s$ and C $2p$ states. The band energy between –6 and –2.1 eV mainly comes from C $2p$, while H $1s$ contributes little in this energy range.

4 Conclusions

To extend our knowledge about the naphthalene under high pressure, we used the density functional theory to study the structural and electronic properties. The variation of the structural quantities, such as cell parameters, volume, and band gap, with increasing pressure does not show any discontinuity up to 30 GPa. This indicates that there is no first-order phase transition for naphthalene up to a pressure of 30 GPa. Moreover, the pressure dependence of the electronic band structure, the total density of states (DOS) and partial density of states (PDOS) of naphthalene were presented. The mechanism responsible for this pressure dependence is analyzed. The calculated results show that there is an energy shift both in conduction and valence band which lead to the band gap reduces smoothly under compression. And near the Fermi level, the valence and conduction bands mainly come from C $2p$ and a strong hybridization can be found between H $1s$ state and C $2p$ state in the conduction band energy between 5.96 and 6.47 eV.

Author contribution statement

Ling-Ping Xiao and Zhi Zeng designed this work. Ling-Ping Xiao wrote the manuscript and prepared all tables and figures. All authors reviewed the manuscript.

This work was supported by NSFC under Grant Nos. 11174284 and U1230202 (NSAF), the special Funds for Major State Basic Research Project of China (973) under Grant No. 2012CB933702, and the Hefei Center for Physical Science and Technology under Grant No. 2012FXZY004.

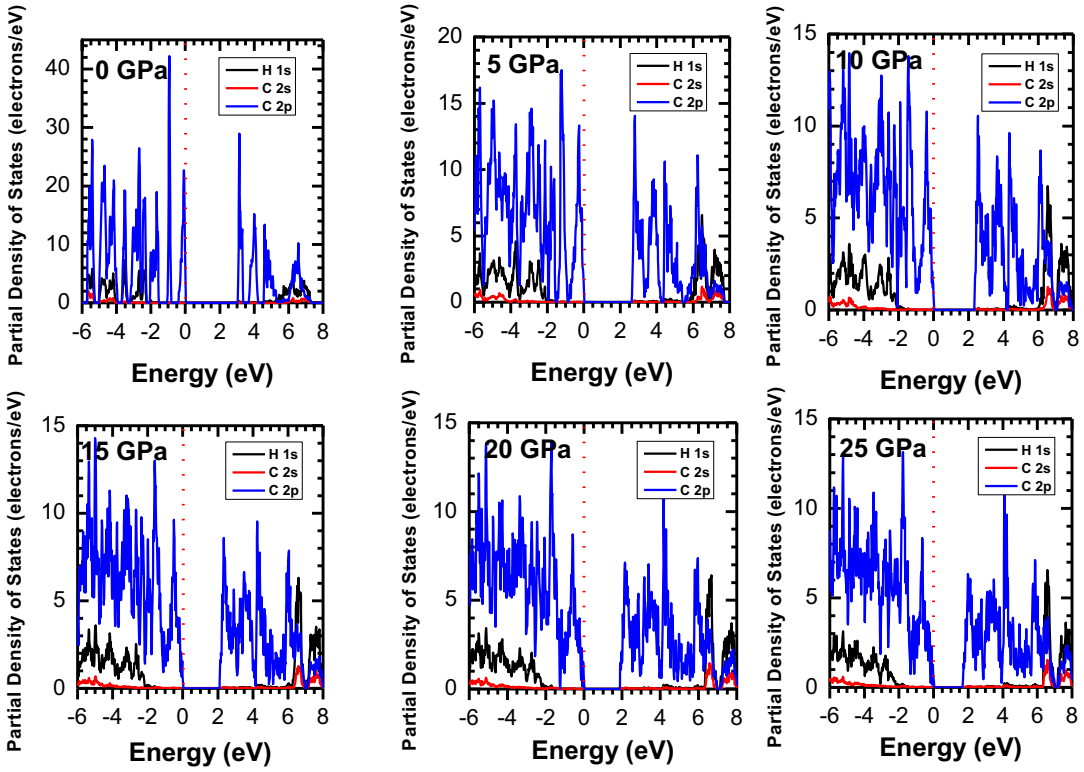

Fig. 7. The partial density of state (PDOS) of naphthalene at 0 GPa, 5 GPa, 10 GPa, 15 GPa, 20 GPa, and 25 GPa, respectively. In each case the Fermi level is indicated by a dashed line.

References

1. E.A. Silinsh, V. Capek, *Organic Molecular Crystals: Interaction, Localization, and Transport Phenomena* (Springer-Verlag, Berlin, Heidelberg, New York, 1994)
2. R. Farchioni, G. Grosso, *Organic Electronic Materials: Conjugated Polymers and Low Molecular Weight Organic Solids* (Springer, Berlin, 2001)
3. L.J. Allamandola, S.A. Sandford, B. Wopenka, Science **237**, 56 (1987)
4. A.I. Kitaigorodsky, *Molecular crystals and molecules* (Academic press, 1973)
5. R.B. Aust, W.H. Bentley, H.G. Drickamer, J. Chem. Phys. **41**, 1856 (1964)
6. Q.W. Huang, G.H. Zhong, J. Zhang, X.M. Zhao, C. Zhang, H.Q. Lin, X.J. Chen, J. Chem. Phys. **140**, 114301 (2014)
7. T. Kambe, X. He, Y. Takahashi, Y. Yamanari, K. Teranishi, H. Mitamura, S. Shibasaki, K. Tomita, R. Eguchi, H. Goto, Y. Takabayashi, T. Kato, A. Fujiwara, T. Kariyado, H. Aoki, Y. Kubozono, Phys. Rev. B **86**, 214507 (2012)
8. I. Harada, T. Shimanouchi, J. Chem. Phys. **44**, 2016 (1966)
9. E.S. Kadantsev, M.J. Stott, A. Rubio, J. Chem. Phys. **124**, 134901 (2006)
10. S. Block, C.E. Weir, G.J. Piermarini, Science **169**, 586 (1970)
11. M.A. McHugh, J.J. Watkins, B.T. Doyle, V.J. Krukonis, Ind. Eng. Chem. Res. **27**, 1025 (1988)
12. G. Heimel, D. Somitsch, P. Knoll, E. Zojer, J. Chem. Phys. **116,** 10921 (2002)
13. K.P. Meletov, Phys. Solid State **55**, 581 (2013)
14. A.Y. Likhacheva, S.V. Rashchenko, A.D. Chanyshev, T.M. Inerbaev, K.D. Litasov, D.S. Kilin, J. Chem. Phys. **140**, 164508 (2014).
15. A.Y. Likhacheva, S.V. Rashchenko, K.D. Litasov, J. Appl. Cryst. **47**, 984 (2014)
16. V. Coropceanu, R.S. Sánchez-Carrera, P. Paramonov, G.M. Day, J.L. Brédas, J. Phys. Chem. C **113**, 4679 (2009)
17. B. Schatschneider, S. Monaco, A. Tkatchenko, J.J. Liang, J. Phys. Chem. A **117**, 8323 (2013)
18. K. Hummer, C. Ambrosch-Draxl, Phys. Rev. B **72**, 205205 (2005)
19. I.A. Fedorov, Y.N. Zhuravlev, V.P. Berveno, Phys. Chem. Chem. Phys. **13**, 5679 (2011)
20. Y.N. Zhuravlev, I.A. Fedorov, M.Y. Kiyamov, J. Struct. Chem. **53,** 417 (2012)
21. G. Kresse, J. Furthmuller, Comput. Mater. Sci. **6**, 15 (1996)
22. K. Lee, E.D. Murray, L. Kong, B.I. Lundqvist, D.C. Langreth, Phys. Rev. B **82**, 081101 (2010)
23. T. Suthana, N. Rajesha, P. Dhanaraja, C. Mahadevan, Spectrochim. Acta Part A **75**, 69 (2010)
24. P.W. Bridgman, Proc. Am. Acad. Arts Sci. **77**, 129 (1949)
25. S. Block, C.E. Weir, G.J. Piermarini, Science **169**, 586 (1970)
26. C.P. Brock, J.D. Dunitz, Acta Crystallogr. B **38**, 2218 (1982)
27. B. Schatschneider, J.J. Liang, A.M. Reilly, N. Marom, G.X. Zhang, A. Tkatchenko, Phys. Rev. B **87**, 060104 (2013)

28. B. Schatschneider, S. Monaco, J.J. Liang, A. Tkatchenko, J. Phys. Chem. C **118**, 19964 (2014)
29. F.P.A. Fabbiani, D.R. Allan, S. Parsons, C.R. Pulham, Acta Crystallogr. B **62**, 826 (2006)
30. A.J. Kitaigorodsky, in *Molekiilkristalle* (Akademie, Berlin, 1979), Vol. 177
31. A.I. Kitaigorodsky, *Molecular Crystals and Molecules* (Academic, New York, 1973)
32. V.A. Venturo, P.M. Felker, J. Chem. Phys. **99**, 748 (1993)
33. H. Saigusa, S. Sun, E.C. Lim, J. Phys. Chem. **96**, 2083 (1992)
34. K. Murata, K. Yokogawa, S. Arumugam, H. Yoshino, Crystals **2**, 1460 (2012)
35. S. Katayama, A. Kobayashi, Y. Suzumura, J. Phys. Soc. Jpn **75**, 054705 (2006)
36. M. Chandrasekhar, S. Guha, W. Graupner, Adv. Mater. **13**, 613 (2001)
37. P.F. Jones, M. Nicol, J. Chem. Phys. **48**, 5440 (1968)
38. M. Nicol, M. Vernon, J.T. Woo, J. Chem. Phys. **63**, 1992 (1975)
39. S.D. Hamann, High Temp. High Pressures **10**, 503 (1978)